

# Characterization of an Ultrasonic Nebulizer–Membrane Separation Interface with Inductively Coupled Plasma Mass Spectrometry for the Determination of Trace Elements by Solvent Extraction†

## Invited Lecture

I. B. BRENNER<sup>\*a</sup>, A. ZANDER<sup>a</sup>, M. PLANTZ<sup>b</sup> AND J. ZHU<sup>c</sup>

<sup>a</sup>Ginzton Research Center, Varian Associates, 3075 Hansen Way, Palo Alto, CA 94305–1025, USA

<sup>b</sup>Varian Optical Spectroscopy Instruments, 201 Hansen Court, Wood Dale, IL 60191, USA

<sup>c</sup>CETAC Technologies, Inc., 5600 South 42nd Street, Omaha, NE 68107, USA

The problems of using an ultrasonic nebulizer–membrane desolvation separation interface (USN–MEMSEP) for the determination of trace elements by solvent extraction and ICP–MS were studied. The interference effects of chloroform and the behavior of trace metal chelates as a function of MEMSEP temperature and sweep gas were studied. In comparison with conventional nebulization, the use of the interface resulted in an approximately 10-fold increase in analyte signals. Although the interface removed much of the chloroform vapor from the aerosol stream by selective permeation and argon counter gas purging, residual solvent resulted in polyatomic ion interferences that affected the limits of detection. The addition of a small flow of oxygen to the auxiliary gas minimized these interferences and prevented carbon deposition on the torch tubes and sampler cones. The  $^{40}\text{Ar}^{12}\text{C}^+$  signal was attenuated, but those of  $^{40}\text{Ar}^{16}\text{O}^+$  and  $\text{CeO}^+/\text{Ce}^+$  increased slightly. An increase in MEMSEP desolvation temperature resulted in a decrease in  $^{35}\text{Cl}^{16}\text{O}^+$  and  $^{40}\text{Ar}^{12}\text{C}^+$  signals due to enhanced rejection of chloroform. Thermal desolvation of the metal organic compound vapors and aerosols resulted in a decrease in the ion counts of the chelated analytes with increasing temperature, probably due to their volatilization and rejection from the membrane. An internal standard could be used to compensate for the responses to changes in temperature. Signal responses of the metal dithiocarbamates to changes in MEMSEP desolvation temperature were significantly different to those in chloroform solutions of oil-based standards, and as a consequence the latter were unsuitable for calibration. The advantages of the technique include matrix elimination, marked reduction in polyatomic carbide ions, enhanced LODs and reduced plasma interferences.

**Keywords:** Inductively coupled plasma mass spectrometry; ultrasonic nebulization; membrane separation; solvent extraction; trace elements

Chemical preconcentration of trace elements by solvent extraction is a convenient approach for improving limits of determination and eliminating interference effects due to bulk chemical constituents. Although methods of solvent extraction have been widely employed with flame spectroscopy,<sup>1,2</sup> the scope of

solvent extraction procedures for analyte preconcentration and matrix elimination with *direct* ICP–MS determination has been constrained owing to the deleterious effects of organic solvent loading on the plasma discharge characteristics. The introduction of volatile solvents into an ICP results in plasma instability due to energy withdrawal, formation of C molecular species such as  $\text{C}_2$ , CN and CO in the plasma, formation of polyatomic ions, and carbon deposition on the torch and sample cone.<sup>3–8</sup> Hence, a system which would allow the *direct* and routine nebulization of volatile solvents into the ICP would greatly increase the prospects for solvent extraction as a method of preconcentration, with the benefits of removal of salt matrices and elimination of spectroscopic and non-spectroscopic interferences.

The effects of organic solvent load have been reduced by addition of oxygen to the plasma, which converts C and the various C-molecular species into CO and  $\text{CO}_2$ .<sup>9,10</sup> The solvent load was minimized using a cooled spray chamber<sup>10–12</sup> and by transporting the heated aerosol produced with an ultrasonic nebulizer (USN) through a desolvating condenser at  $-10^\circ\text{C}$ .<sup>13</sup> It was demonstrated that detection limits improved with decreasing spray chamber and increasing heating stage temperatures. Overloading was also minimized by desolvating the aerosol using crycondensers which were cooled by dry-ice to  $-77^\circ\text{C}$ .<sup>14</sup> Although this desolvation system removed most of the solvent, a significant amount was passed on to the plasma. In a complex arrangement consisting of an ultrasonic nebulizer and multiple heating and cooling cryogenic loops, a larger proportion of volatile organic solvents was removed from the aerosol stream by repetitive heating at  $100^\circ\text{C}$  and cooling with dry-ice and with ethanol at  $-80^\circ\text{C}$ .<sup>15,16</sup> Brotherton *et al.*<sup>12</sup> described a low volume interface for flow injection of volatile solvents into the ICP, consisting of a water cooled mini-spray chamber, a thermal desolvation interface and a partial-suction injector to remove solvent excess by utilizing differences in momentum between aerosol droplets and the solvent vapor. The complications of direct analysis of volatile organics can be inelegantly overcome by back-extracting the analytes into an acidic aqueous solution before ICP analysis.<sup>17–19</sup> This is a time-consuming approach with potential sample contamination.

Gustavsson and co-workers<sup>20,21</sup> developed a membrane interface for ICP–AES to desolvate both aqueous and volatile organic solvents. The membrane separated the nebulizer gas and the aerosol from the the solvent vapors, which were purged

† Presented at the Eighth Biennial National Atomic Spectroscopy Symposium (BNASS), Norwich, UK, July 17–19, 1996.

through the membrane and removed using an argon counter gas. Tao and Miyazaki<sup>22</sup> described a polyimide membrane separator operating at 80 °C to decrease the water loading in an ICP-MS system. As a result,  $^{40}\text{Ar}^{16}\text{O}^+$  and  $^{35}\text{Cl}^{16}\text{O}^+$  decreased by one and two orders of magnitude, respectively, and the  $\text{CeO}^+/\text{Ce}^+$  ratio at the maximum  $^{108}\text{Ce}^+$  signal intensity amounted to 0.11% compared with 11% with their conventional system. Organic solvents were not studied. Botto and Zhu<sup>23</sup> evaluated a commercial USN-membrane desolvation separation interface (MEMSEP) for the analysis of volatile organic solvents using ICP-AES. Approximately 90% of the water mass was removed but only about 30% for various organic solvent vapors. In the case of highly volatile solvents, the efficiency of removal must be high in order to overcome the problems described above.

The extraction chemistry of the combined sodium diethyldithiocarbamate-ammonium tetramethylenedithiocarbamate (pyrrolidine-1-dithiocarbamate) (NaDDC-APDC) system was studied by McLeod *et al.*,<sup>18</sup> Wyttenbach and Bajo<sup>24</sup> and Kinrade and Van Loon.<sup>25</sup> They demonstrated that these chelating agents, used in a ratio of 1:1, permit the selective extraction of numerous transition metals over the pH range 2–6. Citrate or acetate buffers of pH 4–5 were employed, the former being preferred. This extraction system in chloroform and IBMK has been widely applied in flame atomic absorption<sup>1,2,25–28</sup> and in, ETV-AAS,<sup>29</sup> but very rarely using direct injection into the ICP with AES and MS owing to the interferences described above. Thus, Zhuang *et al.*<sup>19</sup> used an elaborate on-line flow injection manifold using Co-APDC coprecipitation for the preconcentration of trace amounts of heavy metals in rain water. Although IBMK dissolved the precipitate, the solvent could not be introduced directly into the plasma. Consequently, the precipitate, collected on a PTFE membrane, was dissolved in nitric acid and hydrogen peroxide and the solution aspirated into the ICP.

In a previous investigation,<sup>30</sup> we examined the feasibility of separating a volatile solvent containing extracted metal chelates using a Cetac (Omaha, NE, USA) ultrasonic nebulizer USN-MEMSEP. Several trace metals were extracted using the Aliquat 336-IBMK extraction system<sup>31,32</sup> and the recoveries determined using ICP-AES. IBMK was aspirated *directly* into the USN to increase the aerosol production efficiency, decrease population of the C-species in the plasma by desolvation and then deliver the organic solvent vapors and aerosols to a thermal membrane desolvator where residual volatile organic components were separated from the metal chelate aerosols. The MEMSEP was operated at 160 °C. The ability of the MEMSEP to separate the volatile organic flows from metal aerosols was demonstrated by determining the recoveries of several transition metals in an oil-based IBMK standard and in the Aliquat 336-IBMK extract relative to an aqueous solution. It was observed that recoveries of several metal chelates were low, evidently owing to volatilization of the organic metal ketonates in either the heating stage of the USN (140 °C) or/and the membrane. The multi-element capability and limits of determination were limited owing to sequential atomic emission detection.

In this investigation, we conducted several experiments to evaluate the interference effects when several metal dithiocarbamates and a multi-element oil-based standard in chloroform was introduced into a USN-MEMSEP. Chloroform (bp about 60 °C) was selected because of its low solubility in water and because most of the solvent would be separated in the interface, resulting in an attenuated solvent load in the plasma. The NaDDC-APDC extraction system was selected owing to its multi-element extraction capability. The effects of membrane desolvation temperature, oxygen and argon sweep gas flow rates were determined.

## EXPERIMENTAL

### Reagents, Purification and Preparation

All plastic and glassware were cleaned by soaking in 20% nitric acid for 24 h, followed by three rinses with ultrapure water. Stock standard solutions (Spex Industries, Edison, NJ, USA) were diluted to produce the tuning solutions and the spiked trace element water samples.

### Extraction Procedure

Chloroform (Fluka, Buchs, Switzerland) was purified by extraction with 50% nitric acid (Select Plus Mallinckrodt, St. Louis, MO, USA); 1 l of chloroform was poured into an acid washed PTFE separating funnel, 100 ml of the acid were added and the mixture shaken for 10 min. The funnel was allowed to stand for 5 min for separation of the acid layer, which was then poured off. This was repeated three times. The chloroform was then washed three times with ultrapure water (18.3 MΩ) (MilliQ Plus Millipore, Bedford, MA, USA.)

In accordance with the results obtained by Kinrade and Van Loon,<sup>25</sup> 1 g of NaDDC (Fluka) and 1 g of APDC (Fluka), dissolved in 200 ml of ultrapure water, were used. These solutions were purified by mock extraction with 10 ml of purified chloroform for 10 min. Citrate buffer was prepared by dissolving 120 g of citric acid and 44 g of sodium citrate in ultrapure water and diluting to 500 ml. The pH was approximately 4. The buffer was purified by extraction with 10 ml of NaDDC-APDC in an acid-washed PTFE separating funnel. A 10 ml volume of purified chloroform was added, mixed for 10 min and allowed to stand for 5 min. The organic layer was separated and discarded. This was repeated three times.

Aqueous solutions containing the trace elements of interest were processed in order to determine the recoveries. The extraction was performed by adding 4 ml of citrate buffer to 200 ml of sample containing 0.1% (v/v) nitric acid, followed by 5 ml of NaDDC-APDC reagent, and agitating the mixture for 10 min and then allowing it to stand for 5 min. A 10 ml volume of purified chloroform was added and the agitation process repeated. The organic layer was then drained and the extraction repeated. The final extraction volume was 20 ml.

### Calibration

Calibration standards were prepared by mixing a multi-element oil-based standard (Spex 21, Spex Industries) with purified chloroform to provide a series of standards containing a blank (chloroform only) and 5, 20, 50 and 100  $\mu\text{g l}^{-1}$  of the trace elements of interest (V, Cr, Mn, Ni, Cu, Fe, Mo, Ag, Zn, Sn, Tl, Cd, Bi and Pb). In order to determine whether these oil-based standards could be used to analyze chloroform extractions, ultrapure deionized water and Canadian National Research Council NAAS-2 sea-water were spiked with 5, 10, 20 and 50  $\mu\text{g l}^{-1}$  of trace metals, processed and analyzed.

### Instrumentation and Operating Conditions

The instrumentation and ICP operating conditions used are listed in Table 1. The chloroform extracts were delivered peristaltically to the USN and removed to the drain using Viton chloroform resistant tubing kits. The USN-MEMSEP interface was a Cetac U-6000AT system consisting of an ultrasonic nebulizer to increase aerosol production efficiency and a 1.5 m microporous tubular PTFE membrane desolvator to remove the organic solvents by a counter flow of argon sweep gas, while the aerosol particles passed through the center of the membrane owing to low permeation and were conveyed to the plasma. The schematic configuration of the MEMSEP and details of its construction were provided by Botto and Zhu,<sup>23</sup>

**Table 1** Instrumentation and ICP operating conditions

Spectrometer	Varian Ultramass
Rf generator	Varian 40.68 MHz
Torch	Demountable, positioned in coil with placement tool
Injector	Alumina, 1.8 mm id
Plasma gas	15.5 l min <sup>-1</sup>
Auxiliary gas	1.1 l min <sup>-1</sup>
Oxygen bleed gas	Varian AGM-1 oxygen supply manifold, 30 ml min <sup>-1</sup>
Rf power	1.2 kW
Depth of sampling	10 mm for aqueous, 6 mm for organic solvents
Sample delivery	1 ml min <sup>-1</sup>
Delivery and drain tubes	Viton; orange for sample, violet for drain
Aerosol carrier flow rate	0.4 l min <sup>-1</sup>
Stabilization time	5 s
Wash-out time	200 s
USN	Cetac U 6000 AT
Desolvation	140 °C
Cooling	Peltier, -10 °C
MEMSEP	CETAC MDX-100
Heating tube	60–160 °C
Sweep gas	0.5–0.7 l min <sup>-1</sup> aqueous; 2 l min <sup>-1</sup> chloroform

Brenner *et al.*<sup>30</sup> and the Cetac instruction manual.<sup>33</sup> MEMSEP operating conditions are listed in Table 1. Data were collected using peak hopping with three points per peak. The measurement time was 1 s, the dwell time 10 ms and the number of replicates three.

The plasma was ignited in the usual way without difficulty. Oxygen was then added slowly to the auxiliary argon gas flow via a T-junction using a Varian (Palo Alto, CA, USA) AGM-1 oxygen delivery manifold (Table 2). Water was then rapidly replaced by propan-2-ol and then by chloroform. The plasma was slowly doped with oxygen until the violet-green C<sub>2</sub> emission surrounding the base and periphery of the plasma and the sampler cone became invisible to the naked eye. The optimum flow rate was 30 ml min<sup>-1</sup>. During this procedure, operator observation of the sampler cone and the torch is essential; an inadequate oxygen flow resulted in the deposition of carbon on the sampler cone, while an excess amount caused its rapid corrosion.

## RESULTS

### Optimization of the ICP-MS System

#### Aqueous solutions

The Varian Ultramass was initially optimized with a concentric pneumatic nebulizer which was then replaced with the USN. In comparison with conventional pneumatic nebulization, the ion intensities obtained with the USN increased by approximately one order of magnitude, while the effect on the background was insignificant. This enhancement is due to higher nebulization efficiencies. The USN–MEMSEP interface was then optimized with an aqueous solution containing 10 µg l<sup>-1</sup> Mg, Co, In, Ce, Th and Pb in 2% v/v nitric acid. With the MEMSEP attached, the relative ion counts of <sup>24</sup>Mg<sup>+</sup>, <sup>59</sup>Co<sup>+</sup>, <sup>115</sup>In<sup>+</sup>, <sup>208</sup>Pb<sup>+</sup> and <sup>232</sup>Th<sup>+</sup> increased by factors of 5–25 (Fig. 1). With a sampling depth of 10 mm, an rf power of 1.2 kW and aerosol and sweep gas flow rates of 0.5 and 0.7 l min<sup>-1</sup>, respectively, the CeO<sup>+</sup>/Ce<sup>+</sup> ratio dramatically decreased from

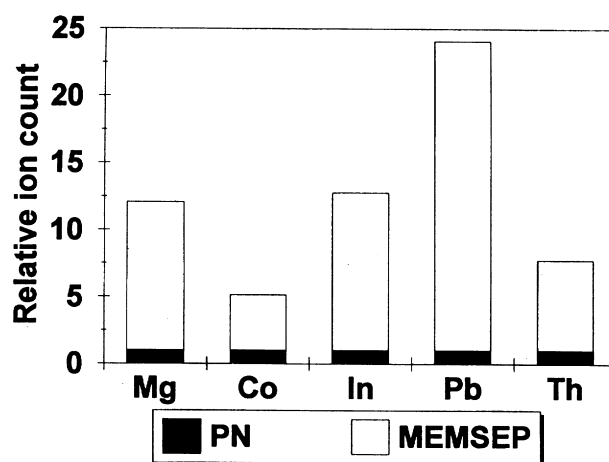


**Fig. 1** Comparison of relative ion counts with and without the MEMSEP. USN attached, aqueous solution.

2–3% to approximately 0.1% and the Ce<sup>2+</sup>/Ce<sup>+</sup> ratio was 0.6%. The reduced oxide ratios are due to low water loading and as a result the desolvated plasma contained more energy which previously was needed to dissociate water molecules.

The effect of the sweep gas flow rate on the ion counts of <sup>24</sup>Mg<sup>+</sup>, <sup>59</sup>Co<sup>+</sup>, <sup>232</sup>Th<sup>+</sup>, <sup>40</sup>Ar<sup>16</sup>O<sup>+</sup> and <sup>108</sup>Ce<sup>+</sup> is illustrated in Figs. 2 and 3. The data in Fig. 2 indicate that the flow rate required to obtain maximum intensity appeared to be mass dependent, the flow rate for <sup>232</sup>Th<sup>+</sup> exceeding those for <sup>24</sup>Mg<sup>+</sup> and <sup>59</sup>Co<sup>+</sup>, implying that the zone of optimum ion intensity for <sup>232</sup>Th<sup>+</sup> was located lower in the plasma. These sweep gas flow rates are higher than those observed in a previous study when the MEMSEP was coupled with ICP-AES.<sup>30</sup> With increasing sweep gas flow rate, <sup>40</sup>Ar<sup>16</sup>O<sup>+</sup> decreased significantly, whereas CeO<sup>+</sup>/Ce<sup>+</sup> passed through a maximum at about 0.75 l min<sup>-1</sup> (Fig. 3).

**Table 2** Plasma ignition routine with USN and MEMSEP attached

Plasma phase	Gas flow rates/l min <sup>-1</sup>			Rf power/ kW	Time/s
	Plasma	Auxiliary	Nebulizer		
Purge	20	2	1	0	30
Delay	20	2	0	0	0
Ignition	18	2	0	0	10
Aspiration	15	1.5	0.8	1–1.2	10

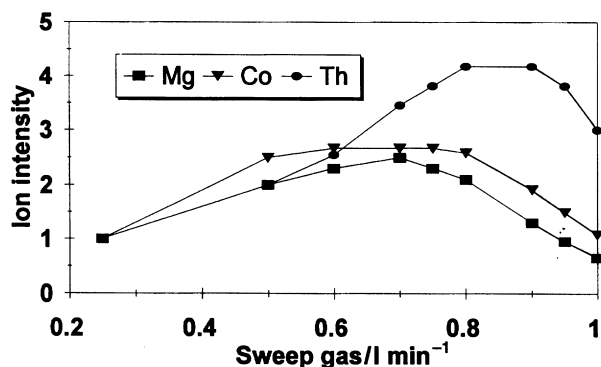


Fig. 2 Effect of sweep gas on  $^{24}\text{Mg}^+$ ,  $^{59}\text{Co}^+$  and  $^{232}\text{Th}^+$  intensities. Aqueous solution with USN-MEMSEP attached.

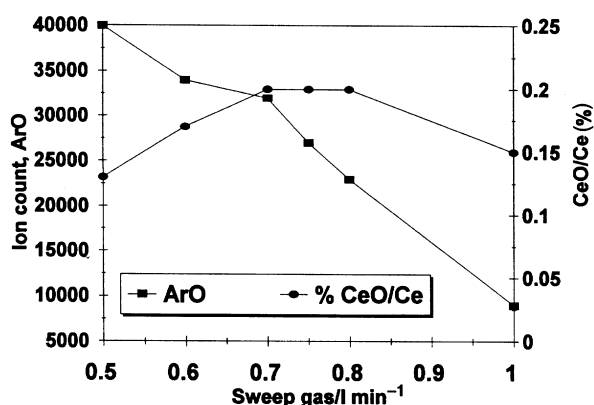


Fig. 3 Variation of  $\text{CeO}^+/\text{Ce}^+$  and  $^{40}\text{Ar}^{16}\text{O}^+$  as a function of the argon sweep gas flow rate. Aqueous solution.

#### Chloroform

The MEMSEP was then optimized with a chloroform-acetone solution containing the analytes mentioned previously using an aerosol flow rate of  $0.4 \text{ l min}^{-1}$ . Despite desolvation, organic gases and vapors were observed in the plasma, and oxygen was introduced into the auxiliary gas flow in order to prevent carbon formation in the torch and on the sampler cone.

#### Effect of oxygen

The effect of oxygen while chloroform was aspirated was determined using an oxygen flow rate of  $30 \text{ ml min}^{-1}$  and a sweep gas flow rate of  $2 \text{ l min}^{-1}$ . A comparison of the relative ion and oxide counts with and without oxygen is illustrated in Fig. 4. While the  $^{140}\text{Ce}^+$  count was not affected by adding oxygen, the  $^{40}\text{Ar}^{12}\text{C}^+$  and  $^{40}\text{Ar}^{12}\text{CH}^+$  signals decreased sharply by a factor of 10, an important benefit for the determination of Cr using  $^{52}\text{Cr}^+$  and  $^{53}\text{Cr}^+$ . The marked decrease in  $^{40}\text{Ar}^{12}\text{C}^+$  is due to the enhanced pyrolysis of chloroform vapor and aerosol. Notwithstanding the addition of oxygen to the plasma, the  $\text{CeO}^+/\text{Ce}^+$  ratio increased only by a factor of 8, probably owing to oxygen consumption in chloroform pyrolysis.

#### Effect of sweep gas

The effect of the sweep gas flow rate on the relative ion counts of  $^{24}\text{Mg}^+$ ,  $^{59}\text{Co}^+$ ,  $^{115}\text{In}^+$ ,  $^{208}\text{Pb}^+$  and  $^{232}\text{Th}^+$  is illustrated in Fig. 5. As in the case of the aqueous solution, the flow rates required to obtain maximum intensity for high mass  $^{208}\text{Pb}^+$  and  $^{232}\text{Th}^+$  were higher than those for  $^{24}\text{Mg}^+$ ,  $^{59}\text{Co}^+$  and  $^{115}\text{In}^+$  when chloroform was aspirated.

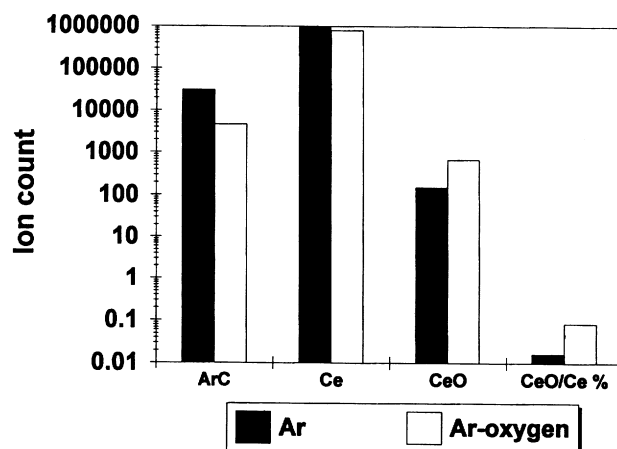


Fig. 4 Effect of oxygen on  $^{40}\text{Ar}^{12}\text{C}^+$ ,  $^{108}\text{Ce}^+$  and  $\text{CeO}^+$ . USN-MEMSEP; oxygen flow rate  $30 \text{ ml min}^{-1}$ ; chloroform.

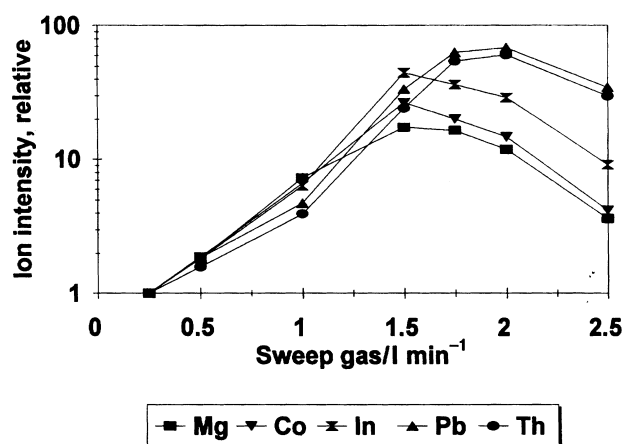


Fig. 5 Effect of sweep gas flow rate on  $^{24}\text{Mg}^+$ ,  $^{59}\text{Co}^+$  and  $^{232}\text{Th}^+$  intensities. Chloroform; oxygen flow rate  $30 \text{ ml min}^{-1}$ ; aerosol flow rate  $0.4 \text{ l min}^{-1}$ .

#### Effect of MEMSEP desolvation temperature

While numerous potential matrix induced interferences were eliminated by solvent extraction (Table 3), numerous C and Cl interferences (Table 4) were observed when chloroform was injected into the MEMSEP at 65 and  $160^\circ\text{C}$ . In particular, high background counts were observed at  $^{51}\text{V}^+$ ,  $^{53}\text{Cr}^+$ ,  $^{56}\text{Fe}^+$ ,  $^{63}\text{Cu}^+$  and  $^{65}\text{Cu}^+$  due to  $^{35}\text{Cl}^{16}\text{O}^+$ ,  $^{37}\text{Cl}^{16}\text{O}^+$ ,  $^{40}\text{Ar}^{16}\text{O}^+$ ,  $^{35}\text{Cl}^{12}\text{C}^{16}\text{O}^+$  and  $^{37}\text{Cl}^{12}\text{C}^{16}\text{O}^+$ , respectively. The desolvation temperature was observed to be a controlling factor in the intensity of C and Cl molecular ions that interfere with these

Table 3 Potential interferences curtailed by applying solvent extraction techniques and membrane separation

Mass	Potential molecular interference
$^{52}\text{Cr}$	$^{40}\text{Ca}^{12}\text{C}$
$^{54}\text{Cr}$	$^{40}\text{Ca}^{14}\text{N}$
$^{55}\text{Mn}$	$^{39}\text{K}^{16}\text{O}$ , $^{23}\text{Na}^{32}\text{S}$
$^{56}\text{Fe}$	$^{40}\text{Ca}^{16}\text{O}$ , $^{39}\text{K}^{16}\text{OH}$ , $^{40}\text{Ar}^{16}\text{O}$ , $^{44}\text{Ca}^{12}\text{C}$
$^{58}\text{Ni}$	$^{40}\text{Ca}^{18}\text{O}$ , $^{23}\text{Na}^{35}\text{Cl}$ , $^{26}\text{Mg}^{32}\text{S}$ , $^{44}\text{Ca}^{14}\text{N}$
$^{60}\text{Ni}$	$^{44}\text{Ca}^{16}\text{O}$ , $^{25}\text{Mg}^{35}\text{Cl}$ , $^{23}\text{Na}^{37}\text{Cl}$
$^{61}\text{Ni}$	$^{44}\text{Ca}^{16}\text{OH}$ , $^{24}\text{Mg}^{37}\text{Cl}$ , $^{23}\text{Na}^{38}\text{Ar}$
$^{62}\text{Ni}$	$^{24}\text{Mg}^{38}\text{Ar}$ , $^{25}\text{Mg}^{37}\text{Cl}$
$^{63}\text{Ni}$	$^{26}\text{Mg}^{37}\text{Cl}$ , $^{24}\text{Mg}^{38}\text{Ar}$ , $^{23}\text{Na}^{40}\text{Ar}$
$^{64}\text{Ni}$	$^{23}\text{Na}^{18}\text{O}$
$^{59}\text{Co}$	$^{24}\text{Mg}^{35}\text{Cl}$ , $^{40}\text{Ca}^{18}\text{OH}$ , $^{43}\text{Ca}^{16}\text{O}$
$^{63}\text{Cu}$	$^{26}\text{Mg}^{37}\text{Cl}$ , $^{23}\text{Na}^{40}\text{Ar}$
$^{64}\text{Zn}$	$^{24}\text{Mg}^{40}\text{Ar}$
$^{66}\text{Zn}$	$^{26}\text{Mg}^{40}\text{Ar}$

**Table 4** Typical interferences due to the presence of chloroform and organic vapors in the aerosol delivered to the plasma

Mass	Molecular interference
$^{51}\text{V}$	$^{35}\text{Cl}^{16}\text{O}$ , $^{32}\text{S}^{18}\text{OH}$
$^{50}\text{Cr}$	$^{32}\text{S}^{18}\text{O}$
$^{52}\text{Cr}$	$^{40}\text{Ar}^{12}\text{C}$ , $^{35}\text{Cl}^{16}\text{OH}$
$^{53}\text{Cr}$	$^{37}\text{Cl}^{16}\text{O}$ , $^{40}\text{Ar}^{12}\text{CH}$
$^{54}\text{Cr}$	$^{35}\text{Cl}^{18}\text{OH}$
$^{60}\text{Ni}$	$^{28}\text{Si}^{32}\text{S}$
$^{63}\text{Cu}$	$^{28}\text{Si}^{35}\text{Cl}$ , $^{12}\text{C}^{16}\text{O}^{35}\text{Cl}$
$^{65}\text{Cu}$	$^{28}\text{Si}^{37}\text{Cl}$ , $^{12}\text{C}^{16}\text{OH}^{37}\text{Cl}$
$^{66}\text{Zn}$	$^{12}\text{C}^{16}\text{OH}^{37}\text{Cl}$

trace metal analytes. For example, Fig. 6 shows the influence of MEMSEP temperature on  $^{40}\text{Ar}^{12}\text{C}^+$ ,  $^{108}\text{Ce}^+$  and  $\text{CeO}^+$  counts when pure chloroform was aspirated. Ce in the inorganic form was employed in order to avoid the possibility of volatilization from the membrane. With increasing temperature from 90 to 160 °C,  $^{40}\text{Ar}^{12}\text{C}^+$  decreased by an order of magnitude owing to the removal of chloroform at high temperature, whereas  $^{108}\text{Ce}^+$  and  $\text{CeO}^+$  remained essentially constant, the latter owing to the absence of water.

In an attempt to devise a universal method of calibration, based on a chloroform solution of oil-soluble metal organic compounds, it was necessary to examine the effect of the desolvation temperature on the signals of several polyatomic ions and analyte masses, and to determine whether the responses are similar for the oil, chloroform and dithiocarbamate matrices. Fig. 7 shows that the intensities of the  $^{35}\text{Cl}^{16}\text{O}^+$  and  $^{40}\text{Ar}^{12}\text{C}^+$  (and  $^{40}\text{Ar}^{12}\text{CH}^+$ ) ions produced by nebulizing dithiocarbamate-chloroform and oil-chloroform solutions decreased by 1–3 orders of magnitude with increasing temperature, the decrease being more prominent between 80 and 90 °C. It should be noted, however, that the signal reductions were not identical for all the matrices.

Fig. 8 shows the abundance corrected net ion counts for an oil-chloroform solution using MEMSEP temperatures of 65 and 160 °C, a 21 min<sup>-1</sup> sweep gas flow rate and the conditions listed in Table 1. In general, the ion signals for 160 °C were lower than those obtained at 65 °C, evidently owing to the volatility of the metal organic compounds used for the preparation of these standards. In detail, Fig. 8 indicates that the 65-to-160 °C signal ratios can be divided into four groups: (a) light elements,  $^{51}\text{V}^+$ ,  $^{52}\text{Cr}^+$ ,  $^{53}\text{Cr}^+$ ,  $^{55}\text{Mn}^+$ ,  $^{58}\text{Ni}^+$ ,  $^{60}\text{Ni}^+$ ,  $^{63}\text{Cu}^+$ ,  $^{65}\text{Cu}^+$ ,  $^{56}\text{Fe}^+$  and  $^{57}\text{Fe}^+$ , with count ratios varying from 15 to about 25; (b)  $^{95}\text{Mo}^+$ ,  $^{96}\text{Mo}^+$ ,  $^{107}\text{Ag}^+$  and  $^{109}\text{Ag}^+$ , with ratios of about 5; (c)  $^{66}\text{Zn}^+$  and  $^{111}\text{Cd}^+$ , which have low

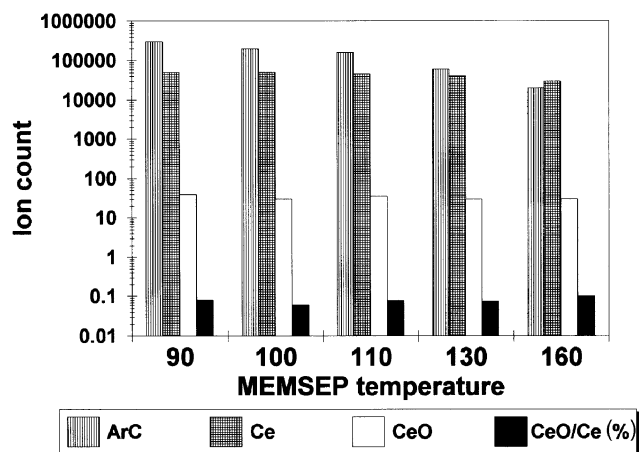


**Fig. 6** Effect of MEMSEP desolvation temperature on  $^{40}\text{Ar}^{12}\text{C}^+$ ,  $^{108}\text{Ce}^+$  and  $\text{CeO}^+$  intensities. Chloroform; sweep gas flow rate 21 min<sup>-1</sup>; aerosol flow rate 0.41 min<sup>-1</sup>.

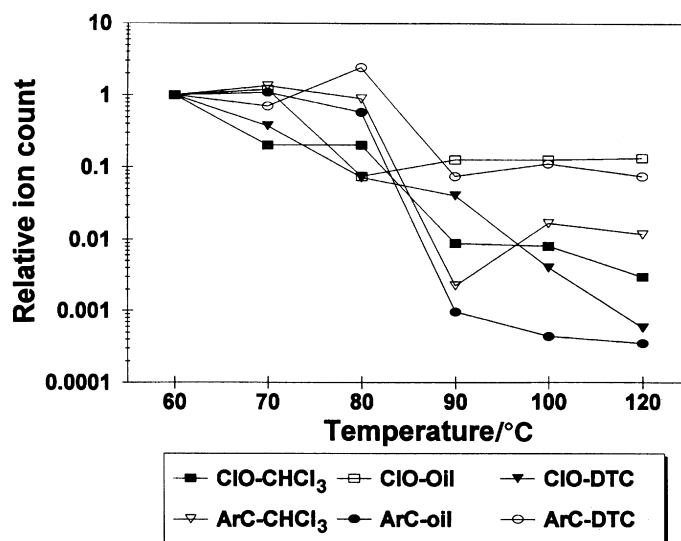


**Fig. 7** Variation of  $^{35}\text{Cl}^{16}\text{O}^+$  and  $^{40}\text{Ar}^{12}\text{C}^+$  as a function of MEMSEP desolvation temperature. Chloroform, chloroform-oil and chloroform-DTCs. Sweep gas flow rate 21 min<sup>-1</sup>; aerosol flow rate 0.41 min<sup>-1</sup>.

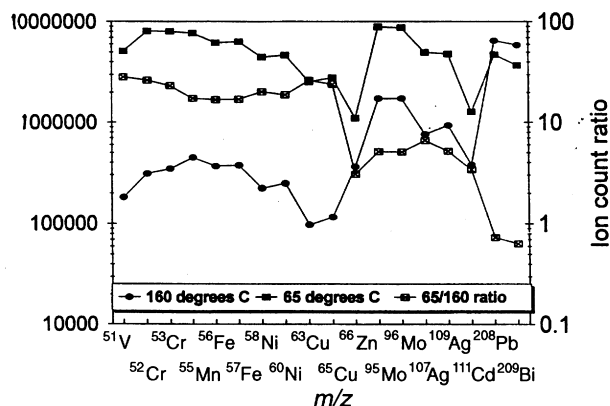


**Fig. 8** Background corrected and abundance normalized intensities for a chloroform-oil solution. MEMSEP temperatures 65 and 160 °C; sweep gas flow rate 21 min<sup>-1</sup>; aerosol flow rate 0.41 min<sup>-1</sup>. Note  $^{66}\text{Zn}^+$  and  $^{111}\text{Cd}^+$  minima.

ratios; and (d) heavy elements,  $^{209}\text{Bi}^+$  and  $^{208}\text{Pb}^+$ , with ratios of about 1. In order to distinguish between ionization and possible volatilization processes, these ratios were plotted as a function of the first ionization potentials (IP) (Fig. 9). Although there is some spread in the relationship between the ratios and IP, Fig. 9 shows that under conditions of moderate plasma overloading, the ion signal of elements that have higher IP ( $^{111}\text{Cd}^+$  and  $^{66}\text{Zn}^+$ ) are more depressed than those that have lower IP. The position of  $^{95}\text{Mo}^+$ ,  $^{107}\text{Ag}^+$ ,  $^{209}\text{Bi}^+$  and  $^{208}\text{Pb}^+$  may reflect their volatilities.

The effect of desolvation temperature on the signals of the metal chelates was evaluated by nebulizing a DDTC-NaDDC extract in chloroform (Fig. 10). Noteworthy was the moderate decrease in the  $^{208}\text{Pb}^+$  signal and the large decrease in  $^{60}\text{Ni}^+$  counts at 60–100 °C. The similar behavior of the other analytes indicates that any one could be employed as an internal standard to compensate for these variations in the USN-MEMSEP interface. It is concluded that metal dithiocarbamates in chloroform are volatilized in the heating stages of the interface. Analyte losses in thermal desolvation devices, especially for those that have high vapor pressures, have been observed frequently in previous studies, *e.g.*, on Hg, B, Os and Re in aqueous solutions and metal dithiocarbamate and keton-

ate complexes.<sup>34</sup> Fig. 11 compares the ion count ratios obtained at 165 and 65 °C for a 20 µg kg<sup>-1</sup> chloroform-oil solution and a dithiocarbamate-chloroform extract. It is evident that the responses for the analytes in these media differ, thus explaining the unsatisfactory recoveries of these elements from

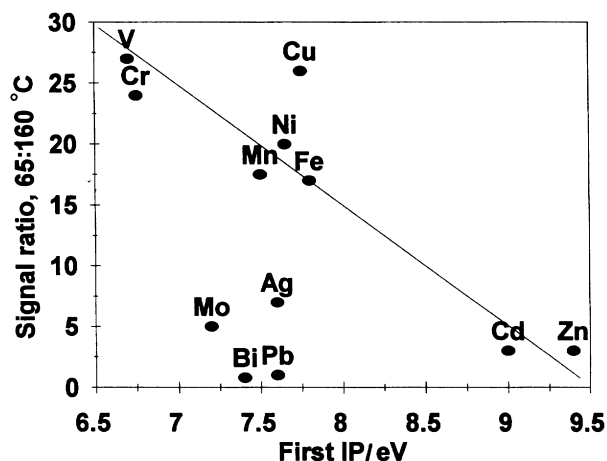


Fig. 9 Relationship between the first ionization potential and the ion count ratios obtained at MEMSEP temperatures of 65 and 160 °C. Chloroform-oil solution; sweep gas flow rate 2 l min<sup>-1</sup>; aerosol flow rate 0.4 l min<sup>-1</sup>; oxygen flow rate 30 ml min<sup>-1</sup>.

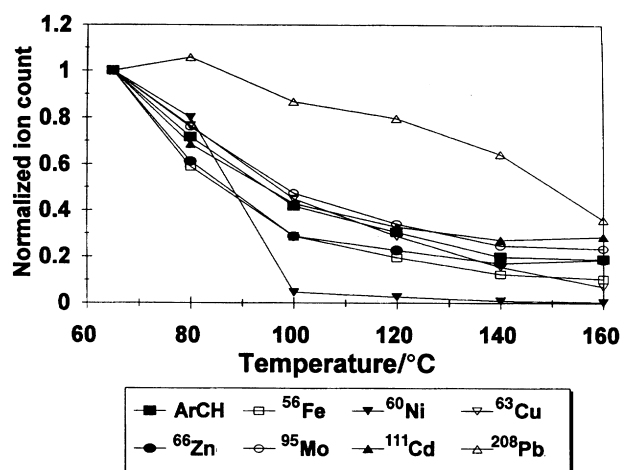


Fig. 10 Effect of MEMSEP desolvation temperature on the ion counts for trace metal dithiocarbamates in chloroform. Sweep gas flow rate 2 l min<sup>-1</sup>; aerosol flow rate 0.4 l min<sup>-1</sup>; oxygen flow rate 30 ml min<sup>-1</sup>.

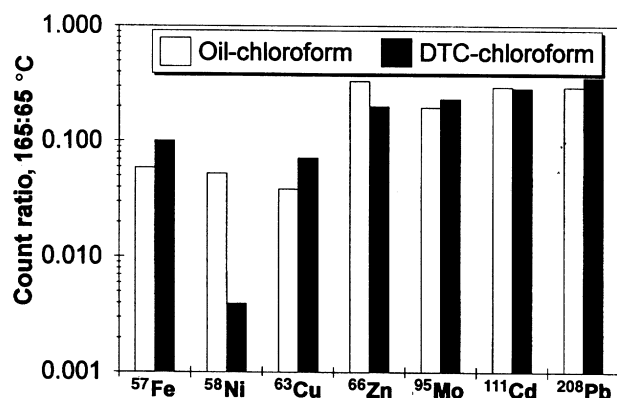


Fig. 11 Response of ion counts obtained at 165 and 65 °C for a 20 µg kg<sup>-1</sup> chloroform-oil solution and a dithiocarbamate-chloroform extract.

spiked water samples and the Canadian sea-water standard NAAS-2.

### Limits of Detection

The 3σ LODs are listed in Table 5. The LODs of <sup>51</sup>V<sup>+</sup> and <sup>52</sup>Cr<sup>+</sup> were constrained by background interferences induced by <sup>35</sup>Cl<sup>16</sup>O<sup>+</sup> and <sup>40</sup>Ar<sup>12</sup>C<sup>+</sup>. The degraded LOD of <sup>56</sup>Fe<sup>+</sup> was due to <sup>40</sup>Ar<sup>16</sup>O<sup>+</sup> and those of <sup>66</sup>Zn<sup>+</sup> and <sup>63</sup>Cu<sup>+</sup> were due to contamination and interferences from <sup>12</sup>C<sup>16</sup>OH<sup>37</sup>Cl and <sup>12</sup>C<sup>16</sup>O<sup>35</sup>Cl. In the case of <sup>63</sup>Cu<sup>+</sup> and <sup>65</sup>Cu<sup>+</sup>, the background increase might also be due to <sup>28</sup>Si<sup>35</sup>Cl<sup>+</sup> formed by thermal ablation of the quartz torch. <sup>118</sup>Sn<sup>+</sup> showed interference by <sup>86</sup>Kr<sup>16</sup>O<sup>+</sup><sub>2</sub>.

### Short-term Variations

The short-term variation was determined by aspirating an oil-chloroform solution into the MEMSEP and recording the intensities over a period of about 120 min (Fig. 12). In general, the accuracy for the 10 µg g<sup>-1</sup> standard varied from -30 to 50%, for 40 µg g<sup>-1</sup> it varied from -28 to 40% and for 100 µg g<sup>-1</sup> it varied from -22 to 28%. More than one internal standard would be required to compensate for these variations.

Table 5 LODs (3σ) in chloroform. Data in µg kg<sup>-1</sup>

Element	LOD/µg kg <sup>-1</sup>
<sup>51</sup> V	0.75
<sup>52</sup> Cr	0.17
<sup>53</sup> Cr	2
<sup>55</sup> Mn	0.011
<sup>56</sup> Fe	0.12
<sup>57</sup> Fe	0.20
<sup>58</sup> Ni	0.042
<sup>60</sup> Ni	0.015
<sup>63</sup> Cu	0.20
<sup>65</sup> Cu	0.22
<sup>66</sup> Zn	0.30
<sup>95</sup> Mo	0.012
<sup>96</sup> Mo	0.007
<sup>107</sup> Ag	0.011
<sup>109</sup> Ag	0.018
<sup>111</sup> Cd	0.015
<sup>118</sup> Sn	0.16
<sup>205</sup> Tl	0.012
<sup>208</sup> Pb	0.002
<sup>209</sup> Bi	0.003

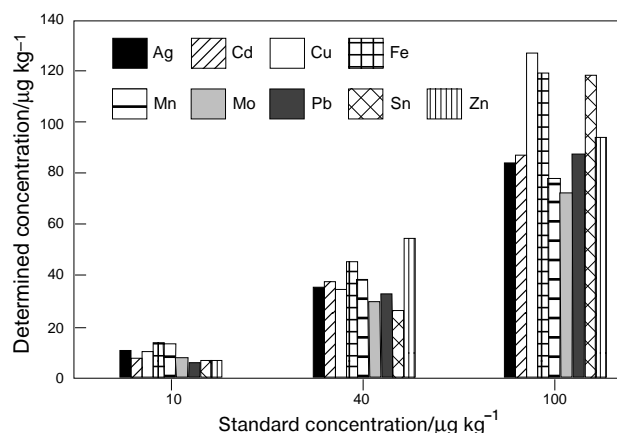


Fig. 12 Short-term accuracy for an oil-chloroform standards (120 min). RSDs were 1–5%.

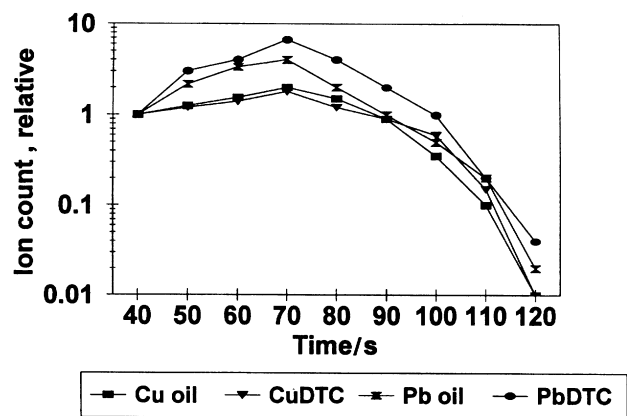


Fig. 13 Memory effect in the USN–MEMSEP interface. Chloroform dithiocarbamate extract (DTC) and oil–chloroform (oil) solution containing  $100 \mu\text{g kg}^{-1}$  of trace elements. Desolvation temperature  $65^\circ\text{C}$ ; seep gas flow rate  $2 \text{ l min}^{-1}$ ; aerosol flow rate  $0.4 \text{ l min}^{-1}$ ; oxygen flow rate  $30 \text{ ml min}^{-1}$ .

### Memory Effects

The memory effect due to possible deposition of analytes in the interface and MS cone was determined using a tuned and calibrated instrument. A  $100 \mu\text{g l}^{-1}$  mixed trace element oil standard and a dithiocarbamate extract, both in chloroform, were aspirated for 120 s. A blank solution was then introduced after 60 s and analyzed after taking into account the time needed for sample uptake. Fig. 13 indicates that the ion count decreased by almost three orders of magnitude after 60 s. This pattern is similar to our previous observations using ICP-AES.<sup>30</sup>

### CONCLUSIONS

The aim of this work was to evaluate interference effects observed when metal chelates and volatile organic solvents are introduced into a USN–MEMSEP ICP–MS interface. On the one hand, the use of high desolvation temperatures results in the efficient removal of interfering organic solvent vapors. On the other hand, operation at high temperature results in the partition of volatile chelates into the USN–MEMSEP interface, depending on the lability of the complexes. In this respect, oil-based standards appear to be unsuitable for universal calibration for the determination of the metal organic species. Because of the volatility of the metal complexes, even at moderate temperatures, the organic solvent used for extraction should have a very low boiling-point. Despite these difficulties, internal standards similar in thermal behavior can be used to compensate for these losses. We are currently evaluating alternative calibration strategies using solvents such as hexane to avoid interferences from  $^{35}\text{Cl}^{16}\text{O}^+$  and calibration standards produced by solvent extraction, and the addition method.

Even though a large amount of the solvent can be removed in the USN–MEMSEP, residual organic vapors and aerosols are introduced into the plasma. Hence a controlled flow of oxygen is necessary to enhance pyrolysis, minimize polyatomic interferences and prevent the deposition of carbon on the torch tubes and sampler cone. By removing matrix elements such as alkali and alkaline earth metals, salt effects are eliminated, and analytes can be preconcentrated provided that their behavior on the membrane interface is well understood. Optimization of the measurement and extraction systems could result in at least 100-fold concentration factors, depending on the amount of sample used and blank contamination.

The technique will be highly suited to HPLC methods which require volatile organic solvents as the mobile phase. In this

case, the MEMSEP would be located between the HPLC column and the ICP. The MEMSEP described in this paper fulfils the requirements of such an interface, namely small memory effects, minimum effects of the mobile phase on the plasma and phase flow rates of  $1\text{--}2 \text{ ml min}^{-1}$ . The technique would also have potential for determining metal organic species in the environment where the integrity of the complex can only be assured by using solvent extraction procedures. Hence we can expect a resurgence of solvent extraction techniques with the use of this USN–MEMSEP interface and ICP–MS.

### REFERENCES

- Cresser, M. S., *Solvent Extraction in Flame Spectroscopic Analysis*, Butterworth, London, 1978.
- Skougstad, M. W., Fishman, M. J., Friedman, L. C., Erdmann, D. E., and Duncan, S. S., in *Techniques of Water-Resources Investigations of the United States Geological Survey*, US Geological Survey, Washington, DC, 1978, ch. A1.
- Boorn, A., and Browner, R. F., *Anal. Chem.*, 1982, **54**, 1402.
- Tang, Y. Q., Du, Y. P., Shao, J. C., Tao, W., and Zhu, M. H., *Spectrochim. Acta, Part B*, 1992, **47**, 1353.
- Maessen, F. J. M. J., Kreunig, G., and Balke, J., *Spectrochim. Acta, Part B*, 1984, **41**, 3.
- Blades, M. W., and Caughlin, B. L., *Spectrochim. Acta, Part B*, 1985, **40**, 579.
- Weir, D. G., and Blades, M. W., *J. Anal. At. Spectrom.*, 1994, **4**, 1323.
- Boorn, A. W., Cresser, M. S., and Browner, R. F., *Spectrochim. Acta, Part B*, 1980, **35**, 823.
- Ohls, K. D., Flock, J., and Loepp, H., *ICP Inf. Newsl.*, 1988, **14**, 83.
- Magyar, B., Lienemann, P., and Vonmont, H., *Spectrochim. Acta, Part B*, 1986, **41**, 27.
- Hausler, D. W., and Taylor, L. T., *Anal. Chem.*, 1981, **53**, 1223.
- Brotherton, T. J., Pfannerstill, P. E., Creed, J. T., Heitkemper, D. T., Caruso, J. A., and Pratsinis, S. E., *J. Anal. At. Spectrom.*, 1989, **4**, 341.
- Botto, R. I., *J. Anal. At. Spectrom.*, 1993, **8**, 51.
- Wiederin, D. R., Houk, R. S., Winge, R. K., and D'Silva, A. P., *Anal. Chem.*, 1990, **62**, 1150.
- Alves, L. C., Wiederin, D. R., and Houk, R. S., *Anal. Chem.*, 1992, **64**, 1164.
- Alves, L. C., Minnich, M. G., Wiederin, D. R., and Houk, R. S., *J. Anal. At. Spectrom.*, 1994, **9**, 399.
- Bradford, G. R., and Bakhtar, D., *Environ. Sci. Technol.*, 1991, **25**, 1704.
- McLeod, C. W., Otsuki, A., Okamoto, K., Haraguchi, H., and Fuwa, K., *Analyst*, 1981, **106**, 419.
- Zhuang, Z., Wang, X., Yang, P., Yang, C., and Huang, B., *J. Anal. At. Spectrom.*, 1994, **9**, 779.
- Gustavsson, A., *Spectrochim. Acta, Part B*, 1987, **42**, 111.
- Backstrom, K., Gustavsson, A., and Hietala, P., *Spectrochim. Acta, Part B*, 198, **44**, 104.
- Tao, H., and Miyazaki, A., *J. Anal. At. Spectrom.*, 1995, **10**, 1.
- Botto, R. I., and Zhu, J. J., *J. Anal. At. Spectrom.*, 1994, **9**, 905.
- Wytenbach, A., and Bajo, S., *Anal. Chem.*, 1975, **47**, 1813.
- Kinrade, J. D., and Van Loon, J. C., *Anal. Chem.*, 1974, **46**, 1894.
- Brooks, R. R., Presley, B. J., and Kaplan, I. R., *Talanta*, 1967, **14**, 809.
- Kojima, I., Inagaki, K., and Kondo, S., *J. Anal. At. Spectrom.*, 1994, **9**, 1161.
- Koirttyohann, S. R., and Wen, J. W., *Anal. Chem.*, 1986, **45**, 1973.
- Sturgeon, R. E., Berman, S. S., Desaulnier, A., and Russell, D. S., *Talanta*, 1980, **27**, 85.
- Brenner, I. B., Zander, A., and Zhu, J., *Fresenius' J. Anal. Chem.*, 1996, **355**, 774.
- Motooka, J. M., *Appl. Spectrosc.*, 1998, **42**, 1293.
- Viets, J. G., *Anal. Chem.*, 1978, **50**, 1097.
- Cetac MDX 100 Membrane Desolvator Instruction Manual*, 1995, Cetac, Omaha, NE.
- Castillo, J. R., Delfa, J., Mir, J. M., Bendicho, C., De la Guardia, M., Mauri, A. R., Mongay, C., and Martinez, E., *J. Anal. At. Spectrom.*, 1990, **5**, 325.

Paper 6/05533H

Received August 8, 1996

Accepted December 5, 1996